engineering proceedings

MDPI

Proceeding Paper

MRI-Based Automated Multi-Class Brain Tumor Classification Using Deep Convolutional Models †

Namratha Sharma [1], Palpandi Subbiah [2,*] and Vijayalakshmi Sankaran [3,*]

[1] Department of Computer Science, Vel Tech Rangarajan Dr. Sagunthala R&D Institute of Science and Technology, Chennai 600062, India; vtd1903@veltech.edu.in
[2] Department of Computer Science and Engineering, Vel Tech Rangarajan Dr. Sagunthala R&D Institute of Science and Technology, Chennai 600062, India
[3] Department of Electronics and Communication Engineering, Vel Tech Rangarajan Dr. Sagunthala R&D Institute of Science and Technology, Chennai 600062, India
* Correspondence: drpalpandis@veltech.edu.in (P.S.); drvijayalakshmis@veltech.edu.in (V.S.)
† Presented at the 13th International Electronic Conference on Sensors and Applications, 18–20 November 2026; Available online: https://sciforum.net/event/ECSA-13.

Abstract

Brain tumors are one of the most life-threatening neurological disorders which is characterized by an anomalous proliferation of cells within the brain that may manifest as either benign or malignant growths. Additionally, the malignant tumors are particularly critical due to their rapid progression and metastatic potential. In this regard, it is essential to diagnose early and accurately for effective therapeutic intervention. Magnetic Resonance Imaging (MRI) remains the gold standard for structural brain visualization; however, the delineation of tumors in a precise manner continues to be a clinical challenge. Also, the conventional diagnostic approaches highly rely on manual radiological interpretation and traditional image processing techniques thereby creates a critical demand for robust computational frameworks. In this work, a deep learning framework for automated brain tumor classification using MRI images from a Kaggle dataset is proposed. Furthermore, the brain images from three different tumors, such as glioma, pituitary, meningioma, and no-tumor brain images are partitioned in 80:20 ratio for the training and testing of deep learning models. The classification is performed using a hybrid Convolutional Neural Network (CNN)-Transformer architecture, EfficientNetV2-B0, DenseNet-121, and Vision CNN with DenseNet121, which are employed and comparatively evaluated for tumor classification. Results demonstrate that the proposed DenseNet 121 model achieves an overall classification accuracy of 93.20% with superior precision, recall, and F1-score standard metrics which significantly outperforms the other three deep learning methods. The proposed work demonstrates the efficacy of deep learning approaches for reliable, interpretable and clinically deployable brain tumor analysis.

Keywords: automated tumor diagnosis; brain tumor detection; clinical decision support systems; computer-aided diagnosis; deep learning; multi-class classification; magnetic resonance imaging

Check for updates

Academic Editor: Stefano Mariani

Published: 13 November 2026

Copyright: © 2026 by the authors. Licensee MDPI, Basel, Switzerland. This article is an open access article distributed under the terms and conditions of the Creative Commons Attribution (CC BY) license.

1. Introduction

A brain tumor is an anomalous evolution of cells in the brain which may be either benign or malignant [1–3], and it disrupts the neural action [4]. Early recognition is crucial for malignant tumors because of their quick development and spreading which lead to serious dysfunction of the neurons [5], with patients commonly presenting seizures, headaches,

vision problems and cognitive deficits [6]. Diagnosis relies on advanced imaging tools, such as MRI, which reveal detailed brain structure [7], though accurate identification remains difficult due to tumor irregularity [8]. Accordingly, advanced computational methods play a crucial role for assisting clinicians with diagnosis and treatment planning [9].

Early detection methods are manual reviews of Computed Tomography (CT) and MRI scans, lengthy methods often resulting in errors [10]. Following this, traditional image pre-processing techniques are introduced such as thresholding and growing regions [11,12]. However, in capturing intricate tumor boundaries, they have lacked accuracy [13]. The advanced machine learning techniques like Fuzzy c-means and k-means clustering were used for detecting and analyzing integral data patterns [14,15]. The advanced deep learning architectures, namely U-Net and CNN, were developed for automatic feature extraction and improving performance by integrating deep learning and clustering techniques which enhance efficient and precise segmentation, outperforming the traditional methods for achieving robustness than prior and better accuracy methodologies [16,17].

EL Badaoui et al. (2025) [11] have proposed a web using a 3D-ATBraTS Deep Learning backend for automatic tumor identification and localization, improving accessibility. Additionally, the authors have used web applications for performing segmentation. Yashini et al. (2025) [12] have proposed an attention-guided framework to classify robustly. The authors have used Grad-CAM to analyze clinical evaluation. Further, the authors have demonstrated that the proposed models such as Convolutional Neural Network (CNN), Residual Network-50 (ResNet-50) and Vision Transformer (ViT) exhibit the threshold points of 3.1 percent. Reddy et al. (2025) [13] have proposed a classification of brain tumors by integrating Multi Res U-Net with adaptation of Inception Net. Additionally, the authors have analyzed comparative evaluation against deep learning models by highlighting F1 score of 97.4384% and Matthew's correlation coefficient of 90.817% which were coupled with the lowest false discovery rate of 3.2514%.

Rana et al. (2025) [14] have proposed a deep learning architecture that combines segmentation and classification models, namely U-Net and CNN, for identifying tumors with high accuracy. Furthermore, the authors have included the segmentation steps that elevated the classification accuracy of 98%. Shoaib et al. (2025) [15] have proposed a deep learning technique for segmenting brain tumors. The model achieves an accuracy of 97% with dice similarity of 92.5% and 92% Intersection Over Union (IOU), which outperforms U-Net and Res U-Net models. Naz and Hameed (2017) [16] have discussed various technologies for the detection of brain tumors and segmentation. Additionally, the authors have described that the MRI images can be considered better-quality inputs for analysis. Abyasa and Rahmania (2025) [17] have introduced AXONS-3 using XAI and 3D U-Net for tumor segmentation. Deepak et al. (2025) [18] proposed normalization, pre-processing and segmentation for tumor analysis, which achieved 83% accuracy. Udupa et al. (2025) [19] proposed an automated deep learning workflow for classification and future extraction.

2. Materials and Methods

2.1. Dataset Collection

The brain tumor MRI dataset was developed by Masoud Nickparvar in January, 2026, and it is publicly available on Kaggle. The dataset consists of four different classes including Glioma, Meningioma, Pituitary and no-tumor class, and contains 7204 human brain MRI images in total; the "no tumor" class images were sourced from the Br35H dataset. Further, the glioma images were taken from the SARTAJ (available on https://www.kaggle.com/datasets/sartajbhuvaji/brain-tumor-classification-mri, accessed on 15 June 2026) and figshare (available on https://figshare.com/articles/dataset/brain_tumor_dataset/1512427, accessed on 15 June 2026). The dataset has two split classifications—testing and training

folders—each further classified into four classes—namely glioma tumor, meningioma tumor, no tumor and pituitary tumor.

2.2. Deep Learning Models

2.2.1. Convolutional Neural Network (CNN)

Convolutional Neural Network (CNN) is a deep learning architecture modeled on the human visual system, designed for grid-structured data like digital images and time-series signals. CNNs automatically extract a hierarchical feature from shallow to complex depths in high-level concepts [20]. The CNN achieves computational efficiency and translation invariance [21]. Convolutional layers detect key features, making the model suitable for pattern recognition, medical image analysis and object detection. The CNN operation is formulated as:

$$O(m,n) = (I * J)(m,n) = \sum_x \sum_y (m+x, n+y) \cdot J(x,y) + P \quad (1)$$

where O is the output value at position (m, n) after applying the convolutional operation, I is the Input image, J represents the convolutional kernel, $\sum_x \sum_y$ represents summation over all kernel elements to compute a single output value and $I(m + x, n + y)$ is the pixel value from the input image.

2.2.2. EfficientNetV2-B0

EfficientNetV2-B0 is a lightweight architecture that combines MBConv blocks and Fused-MBConv blocks with squeeze-and-excitation mechanisms to extract a hierarchical feature. EfficientNetV2-B0 captures both high-level and low-level semantic information while preserving a relatively low computational cost and compact model size that makes it efficient for accurate medical image classification, more specifically for extracting discriminative features from brain MRI scans for the automation of brain tumor classification [22]. EfficientNetV2B0 is formulated as:

$$M_{out} = \sigma(BN(Conv_{k\times k}(M_{in}))) \quad (2)$$

where $\sigma(\cdot)$ denotes nonlinear activation function, M_{in} and M_{out} represent the input and output feature maps, respectively, $Conv_{k\times k}$ denotes the convolution operation with kernel size $k \times k$, and BN denotes batch normalization. The overall architecture integrates MBConv/Fused-MBConv blocks in conjunction with squeeze-and-excitation modules.

2.2.3. DenseNet-121

DenseNet121 is used in classification for its densely connected layers which enhance the vanishing gradient problem and improve accuracy compared to conventional CNNs by connecting layers to each other [23]. DenseNet-121 model addresses this by promoting smooth gradient flow and feature reuse through direct interlayer connections, improving performance in tasks like healthcare image classification. For each dense block, the layer integrates into each previous layer via concatenation formulated as:

$$y_l = H_l([y_0, y_1, ..., y_{l-1}]) \quad (3)$$

where y_l is the output of the l^{th} layer and $H_l(.)$ denotes a composite function. To limit the parameter growth, a bottleneck architecture is used within dense blocks, while the transition layer applies pooling to constrain feature map expansion between two blocks. The final layer uses global average pooling followed by a Softmax classifier to generate output classifiers.

2.2.4. CNN with DenseNet-121

DenseNet-121 is a 121-layer CNN from the Densely Connected Convolutional Network family, with an initial stem, four dense blocks separated by transition layers and a final classification head. The design reduces the vanishing gradients and maximizes feature reuse, allowing DenseNet-121 to match larger networks with far fewer parameters. This makes it efficient for transfer learning tasks like medical image classification [23]. It is formulated as:

$$k_l = T_l([k_0, k_1, k_2, \ldots, k_{l-1}]) \quad (4)$$

where k_l indicates the output feature map of the l^{th} layer, $k_0, k_1, k_2, \ldots, k_{l-1}$ represent the concatenation of feature maps produced by all antecedent layers and T_l indicates a composite non-linear transformation function, typically comprising batch normalization, ReLU activation and convolution.

3. Results and Discussions

Four different deep learning models for brain tumor classification were evaluated and the obtained experimental results are presented in this section. A total of 7204 brain MRI images were used in this study after data augmentation; this set comprises four classes: Glioma (1801 images), Meningioma (1800 images), Pituitary Tumor (1800 images) and No Tumor (1803 images). Furthermore, the dataset was divided into 80% of images being used for training—exactly 5763 images—and 20% for testing—exactly 1441 images. Additionally, the Glioma class had 1441 training and 360 testing images; Meningioma and Pituitary Tumor each had 1440 training and 360 testing images; and the No Tumor class included 1442 training and 361 testing images. Overall, the reliable multiclass brain tumor classification is demonstrated using a CNN. To support a robust and impartial evaluation of the proposed deep neural models, the dataset was segmented into training, testing, and validation subsets. The training set was utilized to refine model parameters, whereas the validation one was utilized to monitor training efficacy, tune the learning rate, employ early stopping, and identify the optimal model checkpoint. Regarding DenseNet121 architecture, transfer learning was carried out using ImageNet-pretrained weights, subsequently fine-tuning the last 50 layers using a decreased learning rate. The study utilized classification accuracy and categorical cross-entropy loss to monitor model training. Upon the completion of training and model selection, the resulting final model was assessed on the confusion matrix, precision, recall, accuracy, and F1-score, which were calculated based on test predictions. The performance of CNN, EfficientNetV2B0, DenseNet121 and CNN with DenseNet121 was assessed using various metrics. Also, the corresponding heatmaps are presented in Figures 1–4. Figure 1 shows the CNN heatmap for four brain MRI classes.

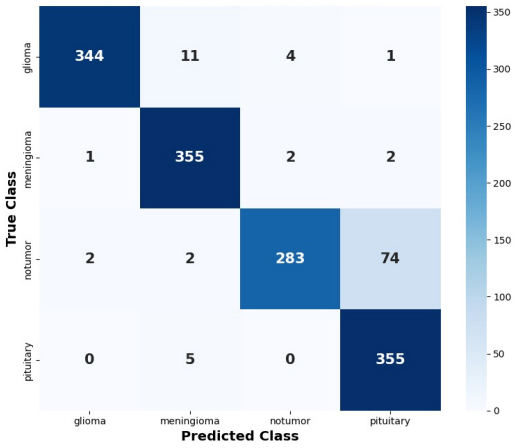


Figure 1. Heatmap of CNN.

Figure 2 illustrates the heatmap of the EfficientNetV2B0 model for the four brain MRI classes. The EfficientNetV2B0 model correctly classified 340 glioma images, 326 meningioma images, 278 no-tumor images and 356 pituitary tumor images. Also, the highest misprediction is observed for the no-tumor class where 78 images were incorrectly classified as pituitary tumor. Similarly, a total of 19 meningioma images were classified as glioma while 14 images were predicted as pituitary tumor. However, even though misclassifications were present, the effective feature extraction is observed with strong diagonal values.

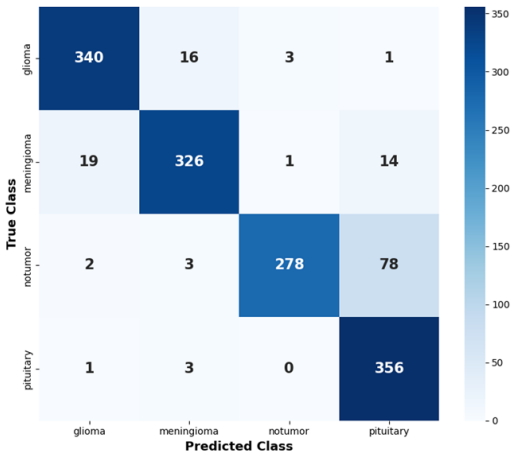


Figure 2. Heatmap of EfficientNetV2B0.

Figure 3 depicts the confusion matrix of the DenseNet121 model for the four brain MRI classes. Furthermore, the model correctly classified 348 glioma, 352 meningioma, 285 no-tumor and 358 pituitary tumor images which demonstrates strong overall prediction performance. Moreover, the pituitary tumor class achieved an accurate classification; however, major confusion occurred in the differentiation between no-tumor images and pituitary tumor images.

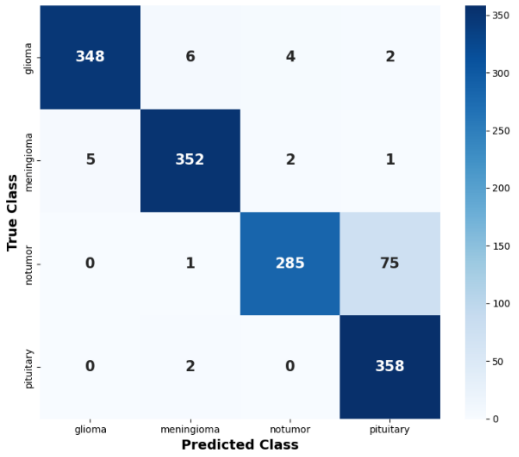


Figure 3. Heatmap of DenseNet121.

Figure 4 shows the heatmap of the CNN with the DenseNet-121 model for the four different brain MRI classes. Also, the model correctly classified 349 gliomas, 331 meningiomas, 277 no-tumor images and 357 pituitary tumors. The no-tumor and pituitary classes achieved strong recognition with minimal false prediction. However, a greater misclassification was observed for gliomas with 53 samples wrongly predicted as meningiomas and 28 as no-tumor images.

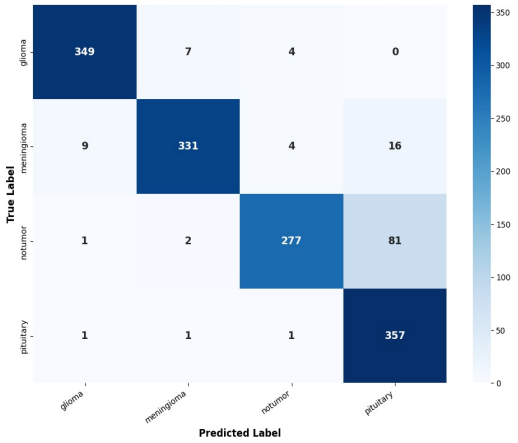


Figure 4. Heatmap of CNN with DenseNet-121.

Table 1 presents the comparative performance of the four different deep learning models for brain MRI classification. Among all the evaluated models, the DenseNet121 achieved the highest overall performance with accuracy of 93.20%, precision of 94.04%, recall of 93.20% and F1_Score of 0.9315. Also, the CNN demonstrated the second-best performance, while the EfficientNetV2B0 achieved a comparatively lower performance. Overall, the DenseNet121 provides robust multiclass classification which demonstrates good discrimination compared to the EfficientNetV2B0, in particular for gliomas, meningiomas and pituitary tumors.

Table 1. Comparative performance of deep learning models for brain MRI classification.

Model	Accuracy (%)	Precision (%)	Recall (%)	F1-Score
CNN	92.78	93.61	92.78	0.9272
EfficientNetV2B0	90.22	91.37	90.22	0.9019
DenseNet121	93.20	94.04	93.20	0.9315
CNN with DenseNet121	91.19	92.38	91.19	0.9118

4. Conclusions

The study presented a deep learning-based framework for automated classification of brain tumors using MRI images. Furthermore, the experimental results demonstrated that all the evaluated models achieved better classification performance. Among all the evaluated models, the DenseNet121 exhibited the best overall performance with an accuracy of 93.20%. It obtained precision of 94.04%, recall of 93.20% and F1_Score of 0.9315. The CNN also demonstrated competitive performance with the accuracy of 92.78%, whereas the EfficientNetV2B0 and the CNN with DenseNet121 obtained accuracy of 91.22% and 91.11%, respectively. Also, the superior performance of DenseNet121 indicates the learning effectiveness of discriminative hierarchical representations from MRI images for multiclass tumor classification. Despite the promising results, some false predictions were observed, especially between the no-tumor and pituitary tumor classes, due to anatomical structures, morphological traits, etc., present in MRI images. The larger and multiple MRI datasets with different geography, advanced image pre-processing, multimodal MRI sequences are planned in the near future to improve clinical interpretability. Overall, the findings establish DenseNet121 as an effective deep learning framework for automated brain tumor classification.

Author Contributions: Conceptualization, N.S., P.S., V.S.; methodology, N.S., P.S., V.S.; software, N.S., P.S., V.S.; validation, N.S., P.S., V.S., N.S., P.S., V.S. and N.S., P.S., V.S.; formal analysis, N.S., P.S., V.S.; investigation, N.S., P.S., V.S.; resources, N.S., P.S., V.S.; data curation, N.S., P.S., V.S.; writing—original draft preparation, N.S., P.S., V.S.; writing—review and editing, N.S., P.S., V.S.; visualization, N.S., P.S., V.S.; supervision, N.S., P.S., V.S.; project administration, N.S., P.S., V.S.; funding acquisition, N.S., P.S., V.S. All authors have read and agreed to the published version of the manuscript.

Funding: This research received no external funding.

Institutional Review Board Statement: Not applicable.

Informed Consent Statement: Not applicable.

Data Availability Statement: The data used in the above study is publicly available in Kaggle. The brain tumor MRI dataset can be retrieved through the following link: https://www.kaggle.com/datasets/masoudnickparvar/brain-tumor-mri-dataset, accessed on 14 June 2026.

Conflicts of Interest: The authors declare no conflicts of interest.

References

1. Rohini, S.; Vidhyasaraswathi, P. A Deep Learning Approach for High-Accuracy Brain Tumor Classification: Evaluating ResNet-50, U-Net, and EfficientNet-B4. In *2025 3rd International Conference on Self Sustainable Artificial Intelligence Systems (ICSSAS)*; IEEE: New York, NJ, USA, 2025; pp. 1366–1373.
2. Choudhary, J.; Kaur, K.; Kumar, A. A Novel Deep Learning-Based Approach for Brain Tumor Segmentation and Classification Using Diffusion-Weighted Imaging and Magnetic Resonance Spectroscopy. In *2025 International Conference on Sustainability, Innovation & Technology (ICSIT)*; IEEE: New York, NJ, USA, 2025; pp. 1–5.
3. Priya; Chandra, M.; Gupta, S. A Review on Advancements in Automatic Brain Tumor detection and classification using Machine Learning Techniques. In *2025 5th International Conference on Advancement in Electronics & Communication Engineering (AECE)*; IEEE: New York, NJ, USA, 2025; pp. 1162–1167.
4. Ünlüleblebici, S.; Kaçmaz, R.N.; Öztürk, C. A Systematic Review of Machine Learning and Deep Learning Techniques for Brain Tumor Classification, and Grading. *IEEE Access* **2026**, *14*, 18075–18098. [CrossRef]
5. Kamala, F.R.; Janardhanan, J.; Gaikwad, B.S.; Annakumari, R.; Nithin, S. A Unified CNN-based System with Grad-CAM for Brain Tumor Segmentation and Classification. In *2025 IEEE 2nd International Conference on Green Industrial Electronics and Sustainable Technologies (GIEST)*; IEEE: New York, NJ, USA, 2025; pp. 1–6.
6. Perkins, A.; Liu, G. Primary brain tumors in adults: Diagnosis and treatment. *Am. Fam. Physician* **2016**, *93*, 211–217B. [PubMed]
7. Rutoh, E.K.; ZhiGuang, Q.; Bore-Norton, J.C.; Bahadar, N. Abi-net: Attention-based inception u-net for brain tumor segmentation from multimodal mri images. *IEEE Access* **2025**, *13*, 134898–134916. [CrossRef]
8. Jayesh, S.; Sophia, S. Multi-Model Deep Learning Framework for Brain Tumor Classification Using MRI and Genomic Data. In *2025 IEEE 4th International Conference for Advancement in Technology (ICONAT)*; IEEE: New York, NJ, USA, 2025; pp. 1–6.
9. Kumaresan, A.; Ibrahim, S.; Guna Ashrin, M. Advancing Brain Tumor Diagnosis: A Machine Learning Approach for Accurate Detection and Classification. In *2025 2nd International Conference on Trends in Engineering Systems and Technologies (ICTEST)*; IEEE: New York, NJ, USA, 2025; Volume 1, pp. 1–6.
10. Kumar, V.D.R.; Singh, P. HCAC: Trustworthy Hybrid Attentive Framework Tackling Brain Tumor Identification with XAI. *IEEE Access* **2026**, *14*, 16158–16175. [CrossRef]
11. El Badaoui, R.; Brainthra, A.; Coll, E.B.; Psarrou, A.; Villarini, B. AI-based System for Brain Tumor Segmentation and 3D Visualization. In *2025 IEEE International Symposium on Circuits and Systems (ISCAS)*; IEEE: New York, NJ, USA, 2025; pp. 1–5.
12. Yashini, P.; Renugadevi, R. Attention-Directed Fusion of Swin Transformer and Radiomic Descriptors to Explainable Classification of Brain Tumor. In *2025 IEEE 4th International Conference for Advancement in Technology (ICONAT)*; IEEE: New York, NJ, USA, 2025; pp. 1–6.
13. Reddy, B.S.; Sathish, A. Attention-Infused U-Net Framework for Robust Brain Tumor Segmentation and Classification. In *2025 Seventh International Conference on Computational Intelligence and Communication Technologies (CCICT)*; IEEE: New York, NJ, USA, 2025; pp. 489–493.
14. Rana, P.; Kashyap, A.; Singh, A.; Patel, A.; Aman, M.; Tyagi, A. Automated Brain Tumor Segmentation and Grade Classification of MRI Using CNN and U-Net. In *2025 5th International Conference on Advancement in Electronics & Communication Engineering (AECE)*; IEEE: New York, NJ, USA, 2025; pp. 1064–1071.
15. Shoaib, M.R.; Niyato, D.; Emara, H.M.; Zhao, J. Automated Segmentation and Classification of Brain Magnetic Resonance Images for Brain Tumor Diagnosis Based on Deep Learning. *IEEE Internet Things J.* **2025**, *13*, 9872–9889. [CrossRef]

16. Naz, S.; Hameed, I.A. Automated techniques for brain tumor segmentation and detection: A review study. In *2017 International Conference on Behavioral, Economic, Socio-cultural Computing (BESC)*; IEEE: New York, NJ, USA, 2017; pp. 1–6.
17. Abyasa, J.; Rahmania, R. AXONS-3: An XAI-Augmented Approach for Advancing Trust and Transparency in 3D Brain Tumor Segmentation. In *2025 IEEE Conference on Cognitive and Computational Aspects of Situation Management (CogSIMA)*; IEEE: New York, NJ, USA, 2025; pp. 64–71.
18. Deepak, H.A.; Jain, B.; Hs, N.F.; Arpitha, U.R.; Prajwal, H.S.; Ayush, S.I. Brain Tumor Classification using MRI Images with CNN and SVM Classifiers. In *2025 5th International Conference on Emerging Research in Electronics, Computer Science and Technology (ICERECT)*; IEEE: New York, NJ, USA, 2025; pp. 1–5.
19. Udupa, B.S.; Gowda, B.; Shashidharan, S.; Ac, P. Brain Tumor Detection and Classification from MRI Using U-Net and Hardware Acceleration. In *2025 IEEE 2nd International Conference on Information Technology, Electronics and Intelligent Communication Systems (ICITEICS)*; IEEE: New York, NJ, USA, 2025; pp. 1–6.
20. LeCun, Y.; Bottou, L.; Bengio, Y.; Haffner, P. Gradient-based learning applied to document recognition. *Proc. IEEE* **1998**, *86*, 2278–2324. [CrossRef]
21. Krizhevsky, A.; Sutskever, I.; Hinton, G.E. Imagenet classification with deep convolutional neural networks. *Commun. ACM* **2017**, *60*, 84–90. [CrossRef]
22. Tan, M.; Le, Q. Efficientnetv2: Smaller models and faster training. In *International Conference on Machine Learning*; PMLR: Cambridge, MA, USA, 2021; pp. 10096–10106.
23. Huang, G.; Liu, Z.; Van Der Maaten, L.; Weinberger, K.Q. Densely connected convolutional networks. In *2017 IEEE Conference on Computer Vision and Pattern Recognition (CVPR)*; IEEE: New York, NJ, USA, 2017; pp. 2261–2269.

Disclaimer/Publisher's Note: The statements, opinions and data contained in all publications are solely those of the individual author(s) and contributor(s) and not of MDPI and/or the editor(s). MDPI and/or the editor(s) disclaim responsibility for any injury to people or property resulting from any ideas, methods, instructions or products referred to in the content.